



Raytheon

ICE SURFACE TEMPERATURE

VISIBLE/INFRARED IMAGER/RADIOMETER SUITE

ALGORITHM THEORETICAL BASIS DOCUMENT

Version 3: May 2000

Yimin Ji
Philip E. Ardanuy

*William Emery, Science Team Member
University of Colorado*

RAYTHEON SYSTEMS COMPANY
Information Technology and Scientific Services
4400 Forbes Boulevard
Lanham, MD 20706

SBRS Document #: Y2405

NPOESS COMPETITION SENSITIVE

EDR: ICE SURFACE TEMPERATURE

Doc No: Y2405

Version: 3

Revision: 0

	Function	Name	Signature	Date
Prepared by	EDR Developer			
Approved by	Relevant IPT Lead			
Approved by	Chief Scientist	P. ARDANUY		
Released by	Program Manager	H. BLOOM		

TABLE OF CONTENTS

	<u>Page</u>
LIST OF FIGURES.....	iii
LIST OF TABLES	iv
GLOSSARY OF ACRONYMS.....	v
ABSTRACT	vi
1.0 INTRODUCTION.....	1
1.1 PURPOSE	1
1.2 SCOPE	1
1.3 VIIRS DOCUMENTS.....	1
1.4 REVISIONS	1
2.0 EXPERIMENT OVERVIEW	2
2.1 OBJECTIVES OF ICE SURFACE TEMPERATURE RETRIEVALS	2
2.2 INSTRUMENT CHARACTERISTICS.....	2
2.3 ICE SURFACE TEMPERATURE RETRIEVAL STRATEGY	4
3.0 ALGORITHM DESCRIPTION	5
3.1 PROCESSING OUTLINE	5
3.2 ALGORITHM INPUT	6
3.2.1 VIIRS Data.....	6
3.2.2 Non-VIIRS Data.....	6
3.3 THEORETICAL DESCRIPTION OF ICE SURFACE TEMPERATURE RETRIEVAL.....	7
3.3.1 Physics of the Problem.....	7
3.3.2 Mathematical Description of the Algorithm	9
3.3.3 Archived Algorithm Output	11
3.3.4 Variance and Uncertainty Estimate.....	11
3.4 ALGORITHM SENSITIVITY STUDIES	15
3.4.1 Calibration Errors.....	15
3.4.2 Instrument Noise	16
3.4.3 Ice Water Mixing	17
3.4.4 Error Budget.....	20

3.5	PRACTICAL CONSIDERATIONS	20
3.5.1	Numerical Computation Considerations	20
3.5.2	Programming and Procedural Considerations	20
3.5.3	Configuration of Retrievals	21
3.5.4	Quality Assessment and Diagnostics	21
3.5.5	Exception Handling	21
3.6	ALGORITHM VALIDATION	21
3.6.1	Pre-Launch Validation	21
3.6.2	Post-Launch Validation	21
3.7	ALGORITHM DEVELOPMENT SCHEDULE	22
4.0	ASSUMPTIONS AND LIMITATIONS	23
5.0	REFERENCES	24

LIST OF FIGURES

	<u>Page</u>
Figure 1. IR radiance at the satellite for five atmospheres simulated by MODTRAN.	3
Figure 2. Atmospheric transmittance for five atmospheres.	3
Figure 3. IST high level flowchart: regression method.....	5
Figure 4. Ice Surface Temperature high level flowchart: physical retrieval.	6
Figure 5. The relationship between temperature deficits at 10.8 μm band and at 12 μm band.	9
Figure 6. The relationship between IST and brightness temperature at the 12 μm band.....	9
Figure 7. Upper panel: Global IST field. Middle panel: The retrieved IST values. Lower panel: The difference between the IST values.	12
Figure 8. IST precision, accuracy, and uncertainty derived from the split window algorithms.	13
Figure 9. IST precision, accuracy, and uncertainty derived from the single band algorithms.	14
Figure 10. Split window IST accuracy related to calibration errors.	15
Figure 11. IST accuracy from global simulation.....	16
Figure 12. Global IST uncertainty for noise free case, and four sensor noise models, derived from testing data.	17
Figure 13. Left panel is the surface temperature derived using IST algorithm, middle is derived from SST algorithm, and the right is the difference	18
Figure 14. Left panel is the surface temperature derived using IST algorithm, middle is derived from SST algorithm, and the right is the difference	19

LIST OF TABLES

	<u>Page</u>
Table 1. Recommended bands and their NEDT values.	4
Table 2. NEDT values in five IR bands for seven sensor noise models.	4
Table 3. IST Error Budget	20

GLOSSARY OF ACRONYMS

ATBD	Algorithm Theoretical Basis Document
ATSR	Along Track Scanning Radiometer
AVHRR	Advanced Very High Resolution Radiometer
CMIS	Conical-Scanning Microwave Imager/Sounder
CrIS	Cross-track Infrared Sounder
ECMWF	European Center for Medium-Range Weather Forecast
EDR	Environment Data Record
IFOV	Instantaneous Field of View
IPO	Integrated Program Office
IR	Infrared
IST	Ice Surface Temperature
LST	Land Surface Temperature
NCEP	National Centers for Environment Prediction
NEDT	Noise Equivalent Delta Temperature
NPOESS	National Polar-orbiting Operational Environmental Satellite System
RMS	Root Mean Square
SBRS	Santa Barbara Remote Sensing
SST	Sea Surface Temperature
TAR	Top Atmospheric Radiance
TOA	Top of Atmosphere
VIIRS	Visible/Infrared Imager/Radiometer Suite

ABSTRACT

This is the Algorithm Theoretical Basis Document (ATBD) for Ice Surface Temperature (IST) retrieval from infrared (IR) signals received by the National Polar-orbiting Operational Environmental Satellite System (NPOESS) Visible/Infrared Imager/Radiometer Suite (VIIRS). IST is a VIIRS level 2 product.

This document describes the theoretical basis and development process of the IST algorithm being developed by the NPOESS algorithm team. The VIIRS IST algorithm will be based on a water vapor correction method. It will utilize radiances from two of the VIIRS far-IR channels. The major error sources for IST retrievals are the atmospheric correction and VIIRS sensor performance. There are a number of difficulties in evaluating the accuracy of satellite estimates of IST. These include the difficulty in distinguishing the snow/ice surface from clouds and the lack of high-quality *in situ* data. Currently, the uncertainty of IST measurements derived from the Advanced Very High Resolution Radiometer (AVHRR) is about 1.5 K.

The VIIRS IST Environment Data Record (EDR) requires a global horizontal cell size of 1 km at nadir with a 1 K measurement uncertainty. Given the VIIRS radiometer noise for IR bands, the total precision for the split window algorithm will be about 0.3 K. In order to meet the 1 K uncertainty requirement, the IST measurement accuracy must be less than 0.95 K. This will require absolute calibration errors of VIIRS far-IR bands of less than 0.5 percent. The VIIRS sensor design will meet this requirement.

Calibration and algorithm validation are the two keys to ensure the performance of the algorithm. Both pre-launch and post-launch activities are discussed in this document. Our current simulations show that the VIIRS IST split window algorithm can meet the VIIRS IST uncertainty requirement. The validation of the VIIRS IST algorithm will strongly depend on the establishment of the matchup database.

The major constraints for the surface temperature algorithm are instrument band selection; instrument Noise Equivalent Delta Temperature (NEDT) for each band; instrument calibration; and the availability and quality of the surface calibration/validation observations.

1.0 INTRODUCTION

1.1 PURPOSE

This is the Algorithm Theoretical Basis Document (ATBD) for the National Polar-orbiting Operational Environmental Satellite System (NPOESS) Visible/Infrared Imager/Radiometer Suite (VIIRS) Ice Surface Temperature (IST) algorithm. In particular, this document identifies sources of input data and describes the theoretical basis and development process of the IST algorithms.

1.2 SCOPE

IST is a VIIRS level 2 product. The IST algorithms described in this ATBD will be used to retrieve IST from VIIRS routinely. Future development efforts may result in modifications to the current operational algorithms. Only algorithms that will be implemented in the operational process are described in this document.

Section 2 of this ATBD provides an overview of the IST algorithm. A description of the algorithm and the development process are presented in Section 3. Section 3 also addresses the error budget, algorithm sensitivity, and validation. Constraints, assumptions, and limitations are discussed in Section 4, and Section 5 presents all citation references in this document.

1.3 VIIRS DOCUMENTS

Reference to VIIRS documents will be indicated by a number in italicized brackets, e.g., *[V-1]*.

[V-1] VIIRS Sensor Requirements Document, NPOESS IPO.

[V-2] VIIRS Sea Surface Temperature Algorithm Theoretical Basis Document (SST ATBD), Raytheon NPOESS Team, SBRS Document # Y2386.

1.4 REVISIONS

This is the third version of this document, dated May 2000. The first version was dated October 1998.

2.0 EXPERIMENT OVERVIEW

2.1 OBJECTIVES OF ICE SURFACE TEMPERATURE RETRIEVALS

Ice Surface Temperature is a crucial component of the Arctic climate. It is a good indicator of the energy balance at the ice surface. The energy exchange between atmosphere and ice layer influences the global climate by controlling the mass balance. A long-term data set of IST can be used to detect and understand the greenhouse effect and climate changes in the polar region. For years the collection of IST has relied on *in situ* measurement from ships, manned ice camps and drifting buoys. The data coverage and our knowledge of the Arctic IST remains poor compared with the other part of the earth's surface.

Although much effort has gone into evaluating the accuracy of satellite measurement of sea surface temperature, there has been no comparable effort for IST. This is due to the considerably greater difficulty in distinguishing the ice surface from clouds and the lack of sufficient high quality *in situ* data. The current rms error of satellite retrieved IST is about 1 to 3 K (Yu *et al.*, 1995; Key *et al.*, 1994). However, the IST has not been retrieved operationally. In general the moisture is lower in the polar atmospheres, although it is considerable in many cases. The IST retrieval methods are split-window statistical methods. Due to the dry air over polar regions, it is also possible to retrieve IST from only one channel within these regions.

The overall scientific objective of the VIIRS IST retrievals is to provide improved measures of global and regional IST fields. The VIIRS IST Environment Data Record (EDR) requires a global horizontal cell size of 1 km at nadir with 1.0 K measurement uncertainty. The uncertainty requirements exceed the current state-of-art results. However, the requirements can be met, provided accurate cloud/ice discriminations. A horizontal cell size of 1.0 km at nadir may be obtained following the current VIIRS design.

2.2 INSTRUMENT CHARACTERISTICS

The VIIRS sensor is being designed based on the NPOESS sensor requirements and EDR thresholds and objectives. Therefore, the following specifications of VIIRS are used only in the current version of retrieval algorithms and are subject to changes during the flowdown process.

VIIRS bands in the far-IR must be placed to optimize their use for surface temperature determination, including Sea Surface Temperature (SST), Land Surface Temperature (LST), and IST. Bands in the far-IR are usually located near the maximum earth radiance. The influence of ozone and other atmospheric absorbers must be avoided. Figure 1 shows the MODTRAN simulated radiance at satellite height for the thermal infrared spectrum. There are a total of five standard atmospheres. There are two regions suitable for far-IR band selection: 8-9 micrometers and 10-13 micrometers. VIIRS far-IR bands will be located in these two regions. Bands in the far-infrared also need to be placed where the atmosphere is most transparent. Figure 2 shows the MODTRAN simulated atmospheric transmittance for five standard atmospheres. It shows that the 10-13 micrometer region is one of the most transparent atmosphere windows for arctic atmospheres.

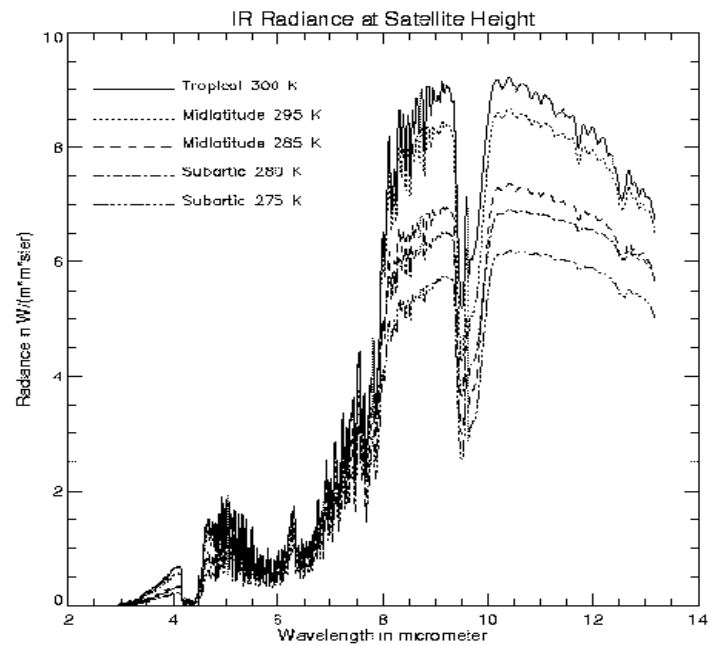


Figure 1. IR radiance at the satellite for five atmospheres simulated by MODTRAN.

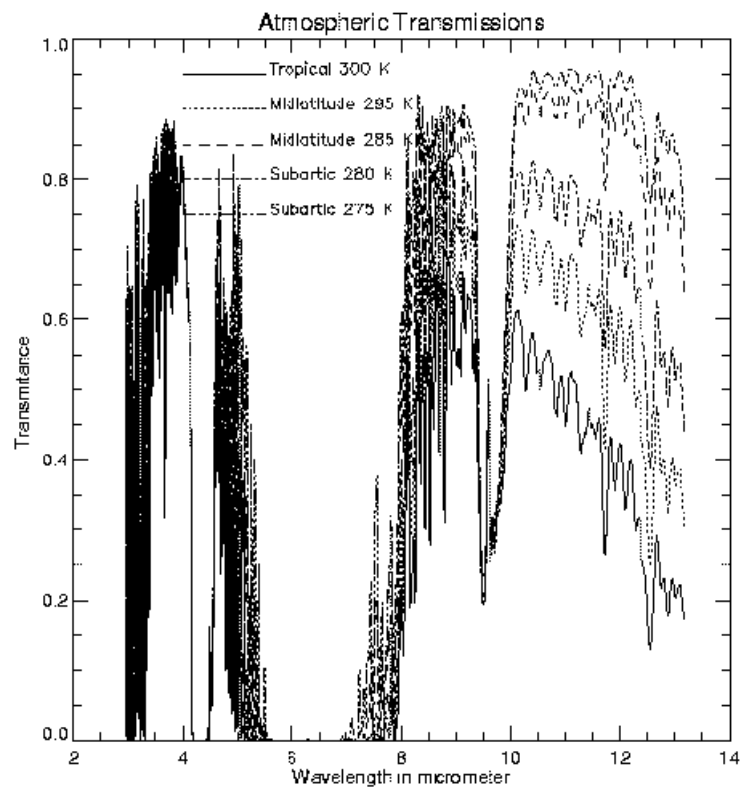


Figure 2. Atmospheric transmittance for five atmospheres.

In the current version of the sensor design, two bands will be used for IST retrievals. The specifications for the two bands are listed in Table 1. The specifications of these bands are similar to those presently in use.

Table 1. Recommended bands and their NEDT values.

λ (μm)	$\Delta\lambda$ (μm)	IFOV(km)		Detector Type	NEDT(K) (At 300K)
		Nadir	EOS		
10.8	1	0.742	1.094	PV HgCdTe	0.038
12	1	0.742	1.094	PV HgCdTe	0.070

Table 2 shows the NEDT values for seven sensor noise models in the two bands. These models have been used to drive sensor design and algorithm development.

Table 2. NEDT values in five IR bands for seven sensor noise models.

λ (μm)	$\Delta\lambda$ (μm)	NEDT(K at 300 K)/Aperture Diameter (cm)						
		Model 1 29 cm	Model 2 24 cm	Model 3 19 cm	Model 4 14 cm	Model 5 9 cm	Model 6 4 cm	Model 7 1 cm
10.8	1	0.04	0.06	0.08	0.13	0.30	1.43	20.88
12	1	0.05	0.07	0.10	0.17	0.38	1.85	26.92

There are 16 suggested bands for VIIRS. These bands will be used to retrieve cloud cover/layers and cloud/ice surface discriminations that are critical to the IST retrieval.

2.3 ICE SURFACE TEMPERATURE RETRIEVAL STRATEGY

Before IST retrievals can be performed within a given region, various atmospheric and surface parameters need to be determined. A cloud cover mask and a Snow/Ice mask will be used to eliminate cloud contaminated or land or ocean water covered pixels. The IST algorithms are run only under clear sky conditions. The following sequence of IST retrieval activity is performed on all suitable pixels within a region. First, the brightness temperatures are calculated for the two bands. ISTs will be calculated using regression equations. The results will be aggregated to the required horizontal cell size.

3.0 ALGORITHM DESCRIPTION

3.1 PROCESSING OUTLINE

There are two IST retrieval methods: the physically based, or ATSR-like, regression method; and the physical method. Regression methods are assisted by the establishment of ancillary data and radiative transfer models initially. The coefficients of regression equations will be obtained from simulation processes. Figure 3 depicts the processing concept for statistical IST retrieval. Physical retrieval involves inversion of the solution to the radiative transfer equation to convert Top of Atmosphere (TOA) to IST. Physical retrieval obtains skin temperature. Figure 4 shows the flow chart for physical retrievals. Physical retrieval will be used only to retrieve 30 km resolution IST fields.

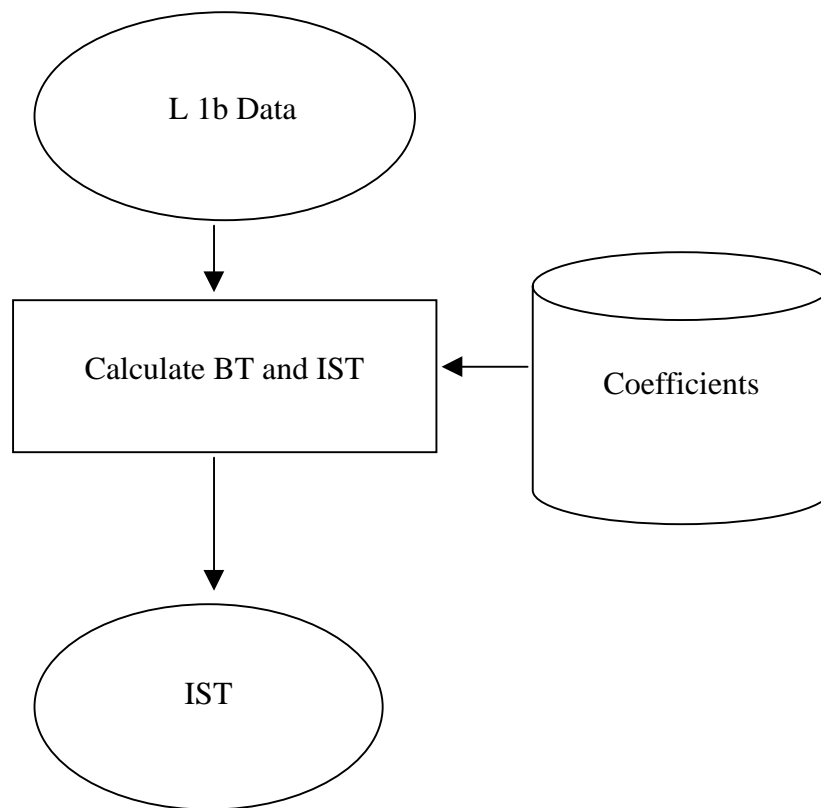


Figure 3. IST high level flowchart: regression method.

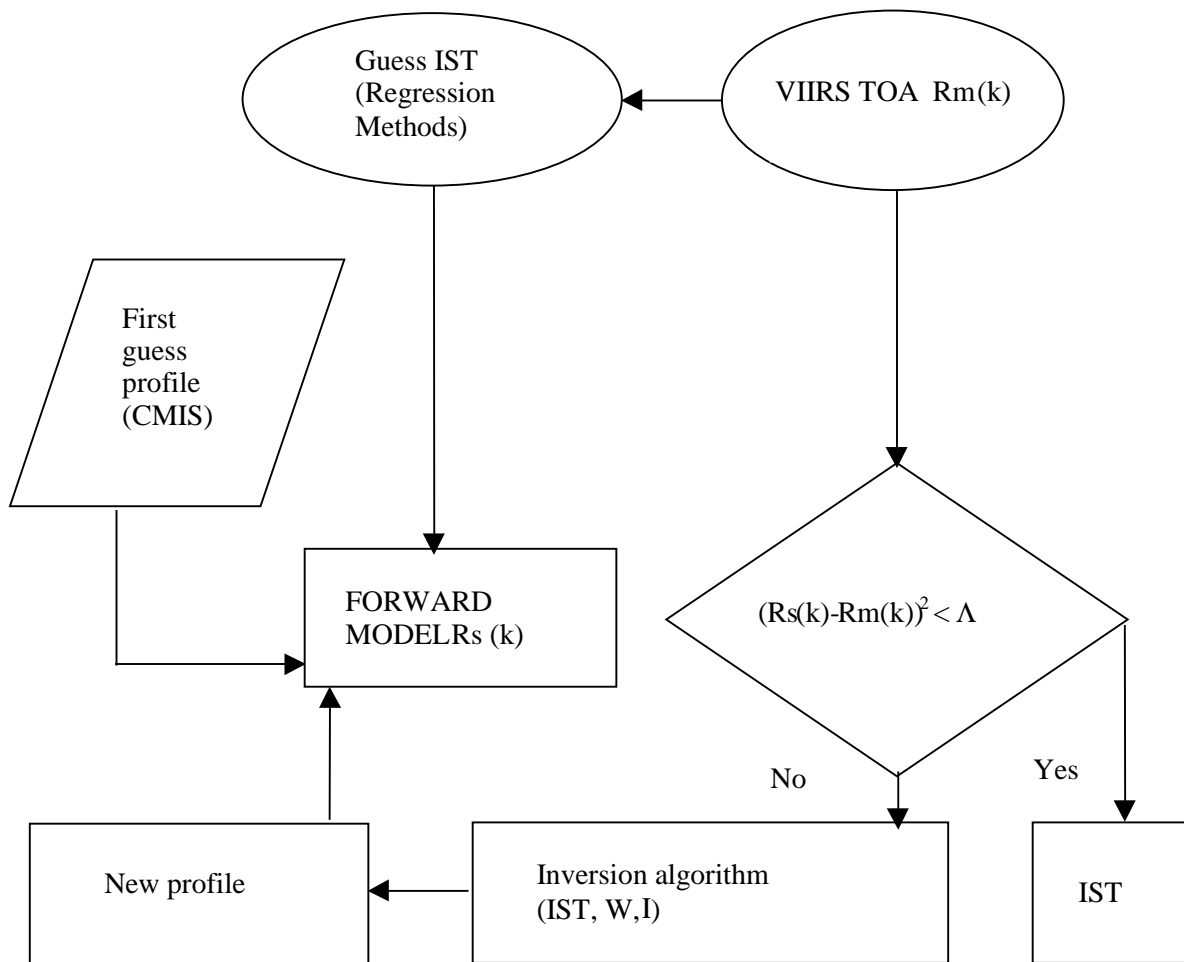


Figure 4. Ice Surface Temperature high level flowchart: physical retrieval.

3.2 ALGORITHM INPUT

3.2.1 VIIRS Data

Required inputs for the IST retrieval to be obtained from VIIRS data stream are: Cloud Mask, Ice Concentration, and Level 1b georectified radiance products.

3.2.2 Non-VIIRS Data

Inputs are required for the IST retrieval that are outside the VIIRS data stream. These include: Land/Ocean Mask, observed and analyzed skin IST, Conical-Scanning Microwave Imager/Sounder (CMIS), and Cross-track Infrared Sounder (CrIS) atmospheric profiles.

3.3 THEORETICAL DESCRIPTION OF ICE SURFACE TEMPERATURE RETRIEVAL

3.3.1 Physics of the Problem

In clear sky conditions, the outgoing infrared spectral radiance at the top of atmosphere can be represented by:

$$L(\lambda, \mu) = \tau(\lambda, \mu)\varepsilon(\lambda, \mu)B(\lambda, T_s) + L_a(\lambda, \mu) + L_s(\lambda, \mu, \mu_0, \varphi_0) + L_d(\lambda, \mu, \mu_0, \varphi_0) + L_r(\lambda, \mu, \mu_0, \varphi_0) \quad (1)$$

Where τ is the transmissivity, ε the surface spectral emissivity, B the Plank function, L_a the thermal path radiance, L_s the path radiance resulting from scattering of solar radiation. L_d is the solar radiance and L_r the solar diffuse radiation and atmospheric thermal radiation reflected by the surface. λ is the wavelength. $\mu = \cos(\theta)$, $\mu_0 = \cos(\psi)$, where θ is the satellite zenith angle, ψ the solar zenith angle. φ_0 is azimuth angle.

The wavelength is the wavelength center of a narrow interval because there is no way to measure the exact monochromatic signal as a continuous function of wavelength by satellite sensors. Equation 1 can be used in the 3-14 μm range. It requires complete calculations of the atmospheric radiative transfer to determine the values of all terms on the right side. This equation has been used in many atmospheric radiation models including LOWTRAN (Kneizys *et al.*, 1988), MODTRAN (Berk *et al.*, 1987), and MOSART (Cornette *et al.*, 1994).

It has been noted that satellite infrared radiance can be corrected straightforwardly for atmospheric absorption in the water vapor bands by utilizing a split window technique. In the following discussion, we outline a theoretical basis for the split window method. This method can be extended to multi-bands methods in nighttime.

For far-IR bands, L_d , L_s and L_r are negligible. Therefore, only the first two terms on the right side of the above equation are important. In this case, if we ignore the change of emissivity over the ocean, the radiance error introduced by the atmosphere ΔL can be represented by:

$$\begin{aligned} \Delta L &= B(\lambda, T_s) - L(\lambda, \mu) = B(\lambda, T_s) - \tau(\lambda, \mu)B(\lambda, T_s) - L_a(\lambda, \mu) \\ &= - \int_1^{\tau(\lambda, \mu)} B(\lambda, T_s) d\tau(\lambda, \mu, p) + \int_1^{\tau(\lambda, \mu)} B(\lambda, T_p) d\tau(\lambda, \mu, p) \\ &= - \int_1^{\tau(\lambda, \mu)} (B(\lambda, T_s) - B(\lambda, T_p)) d\tau(\lambda, \mu, p) \end{aligned} \quad (2)$$

From the Planck function we find:

$$\Delta L = \frac{\partial B}{\partial T} \Delta T = \frac{\partial B}{\partial T} (T_s - T_\lambda) \quad (3)$$

For an optically thin gas the following approximations can be made:

$$d\tau = d\{exp(-k\lambda L)\} = -k\lambda dl \quad (4)$$

Where k_λ is the absorption coefficient and l is the optical path-length. If we assume that the Planck function is adequately represented by a first order Taylor series expansion in each channel window, then:

$$B(\lambda, T_s) - B(\lambda, T_p) = \left. \frac{\partial B(\lambda, T_p)}{\partial T} \right|_{T_s} (T_p - T_s) \quad (5)$$

Substituting Equations 3, 4, 5 into Equation 2, we obtain:

$$T_s - T_\lambda = k_\lambda \int_1^\tau (T_s - T_p) dl \quad (6)$$

Therefore, if we pick two spectral regions of the atmosphere, we will have two linear equations with different k_λ to solve simultaneously.

For example, if we consider two channels as $\lambda=1$ and $\lambda=2$, then we get:

$$T_s - T_1 = -(T_s - T_2)k_1/k_2 \quad (7)$$

Figure 5 shows the relationship between $T_s - T_{11}$ and $T_s - T_{12}$ from MODTRAN simulations. The brightness temperature at the 10.8 μm (T_{11}) band is higher than that at the 12 μm band (T_{12}). However, the relationship between $T_s - T_{11}$ and $T_s - T_{12}$ is rather linear. The maximum difference is only about 3 K.

In general, the ice surface temperature can be represented as:

$$\mathbf{T}_s = \mathbf{C}\mathbf{T}_b \quad (8)$$

The coefficient vector \mathbf{C} , relating observed brightness temperatures to IST, is determined using regression methods by solving:

$$\mathbf{C} = \mathbf{Y}\mathbf{X}^T(\mathbf{X}\mathbf{X}^T + k\mathbf{I})^{-1} \quad (9)$$

The \mathbf{Y} matrix contains a large number of training IST, and the \mathbf{X} matrix contains brightness temperatures from VIIRS far-IR channels. In general, the \mathbf{X} matrix may include non-linear terms.

Because the atmospheric correction term is small, it is possible to use only one channel to retrieve IST. Figure 6 shows the relationship between IST and the brightness temperature at the 12 micrometer band. The relationship is linear.

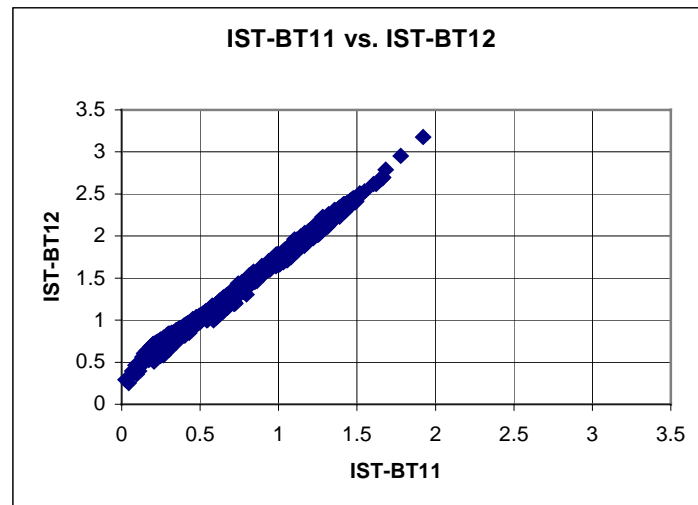


Figure 5. The relationship between temperature deficits at 10.8 μm band and at 12 μm band.

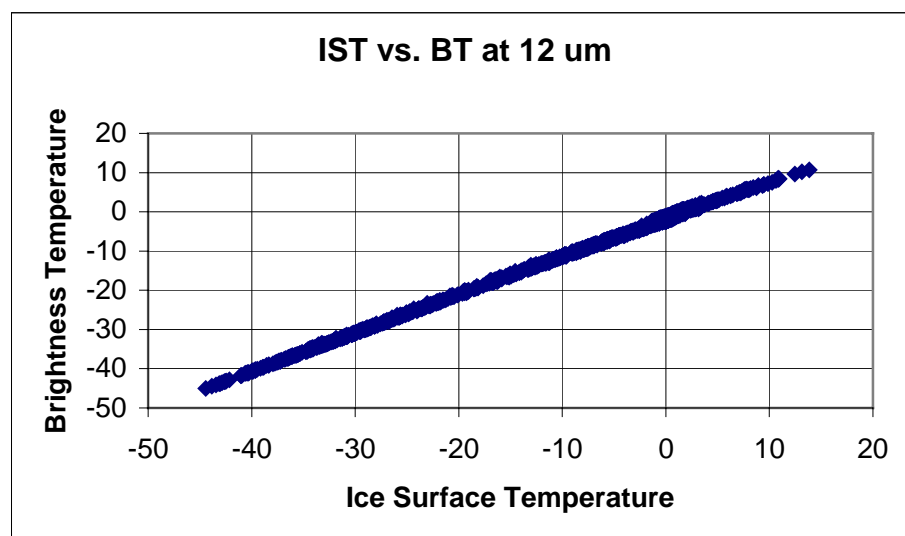


Figure 6. The relationship between IST and brightness temperature at the 12 μm band.

Currently, the IST uncertainty from the regression algorithm is about 1 to 3 K. Since the atmosphere over ice surface is usually dry, it is possible to use only one channel to retrieve IST.

3.3.2 Mathematical Description of the Algorithm

The VIIRS IST algorithm is based on statistical methods. Traditional statistical methods for satellite IST retrieval are linear multi-channel regression methods. The following regression methods are used in the VIIRS IST retrieval:

Split window (10.8 + 12 μm bands, from AVHRR method, Yu *et al.*, 1995):

$$IST = a_0 + a_1 T_{11} + a_2 (T_{11} - T_{12}) + a_3 (\sec(z) - 1) \quad (10)$$

One channel (12 μm band):

$$IST = a_0 + a_1 T_{11} + a_2 (\sec(z) - 1) \quad (11)$$

The second method can be used to retrieve very high resolution IST fields (300 m at nadir).

Satellite-measured radiance is a function of the atmospheric profiles and surface properties. For the IR window and water vapor channels, the radiance over oceans at the top of the atmosphere is mainly a function of the surface temperature and the temperature and moisture profiles. One can choose a few channels (e.g., 3 channels) for which only the main structures of the temperature and moisture profiles are required to obtain sea surface temperature. The main structure for the mixing ratio $q(p)$ of water vapor may be described by a power law.

$$q(p) = g(\alpha + 1)W / p_0 (p / p_0)^\alpha \quad (12)$$

where g is the acceleration of gravity, W is total column water vapor, p is the atmospheric pressure, and p_0 is the atmospheric pressure at the surface. The satellite-measured radiance at channel k can be approximately expressed as:

$$\begin{aligned} R_k &= f_k(W, T_s, \alpha) + \varepsilon'(k) \\ &= R_k^0 + \frac{\partial f_k}{\partial W} \Delta W + \frac{\partial f_k}{\partial T_s} \Delta T_s + \frac{\partial f_k}{\partial \alpha} \Delta \alpha + \varepsilon(k) \end{aligned} \quad (13)$$

where $\varepsilon(k)$ is the total error due to the above assumption and the sensor noise, R_k^0 is the radiance for the present atmospheric state, and T_s is surface temperature. By applying 3 channels, one can have 3 equations. Thus, an inversion equation can be written as:

$$\Delta \mathbf{P} = [\mathbf{A} \mathbf{A}^T + \varepsilon]^{-1} \mathbf{A}^T \Delta \mathbf{R} \quad (14)$$

where:

$$\Delta \mathbf{P} = \begin{bmatrix} \Delta W \\ \Delta T_s \\ \Delta \alpha \end{bmatrix}, \Delta \mathbf{R} = \begin{bmatrix} R_1 - R_1^0 \\ R_2 - R_2^0 \\ R_3 - R_3^0 \end{bmatrix}, \mathbf{A} = \begin{bmatrix} \frac{\partial f_1}{\partial W} & \frac{\partial f_1}{\partial T_s} & \frac{\partial f_1}{\partial \alpha} \\ \frac{\partial f_2}{\partial W} & \frac{\partial f_2}{\partial T_s} & \frac{\partial f_2}{\partial \alpha} \\ \frac{\partial f_3}{\partial W} & \frac{\partial f_3}{\partial T_s} & \frac{\partial f_3}{\partial \alpha} \end{bmatrix} \quad (15)$$

\mathbf{A}^T is the transpose of matrix \mathbf{A} , and ε is an error matrix.

This physical retrieval method is adopted from VIIRS Sea Surface Temperature (SST) retrieval [V-2].

3.3.3 Archived Algorithm Output

Brightness temperatures at 1.0 horizontal cell size are computed for all VIIRS far-IR bands for all satellite viewing angles. The best IST estimates are archived. The magnitude of the uncertainties are also calculated.

3.3.4 Variance and Uncertainty Estimate

The IST retrieval uncertainty is determined by two factors: atmospheric correction and sensor performance. There are a number of error sources in sensor performance. Among them, sensor noise, calibration error, geolocation, and band-to-band registration are the apparent error sources for IST retrieval. Another source of uncertainty is the nature of the ice surface. Snow cover and melt ponds observed elsewhere can drastically change the IST. Because calibration does not contribute to retrieval precision, we will first consider sensor noise.

The data set used to estimate the IST uncertainty and accuracy is a global snapshot surface temperature at 2.5° by 2.5° resolution supplied by National Centers For Environment Prediction (NCEP), with matching atmospheric profiles. The data were used to simulate the top atmospheric radiance (TAR). The noises were added to the TAR through the Santa Barbara Remote Sensing (SBRS) sensor noise models.

In Figure 7, the upper panel shows the global snapshot IST at 00Z July 1, 1993 and the middle panel shows the retrieved IST. The lower panel shows the difference. The NEDT values are about 0.1 K for split windows (SBRS sensor noise model 3). The root mean square (RMS) error is about 0.16 K at this noise level without considering any absolute calibration errors. The maximum error is 0.74 K in daytime and 0.46 K in nighttime.

The retrieval error is a function of satellite viewing angles and surface temperature values. In Figure 8, the upper panel shows the IST precision as a function of satellite zenith angle and surface temperature. The 0.2 K absolute calibration error was considered in this retrieval. The algorithm used is the split window regression method. The precision error is less than 0.3 K for most satellite zenith angles and temperatures. The middle panel shows the IST accuracy error.

The accuracy is generally better than 0.2 K. The lower panel shows the RMS error. The RMS error is less than 0.3 K for higher temperatures and most of the satellite viewing angles. For large zenith angles and lower surface temperatures, the uncertainty is larger, but still less than 0.5 K.

Figure 9 shows the IST precision, accuracy and uncertainty from the single band algorithm. The errors are larger in this algorithm than that in the split window algorithm. But the errors are still less than 0.5 K, except for large satellite viewing angles.

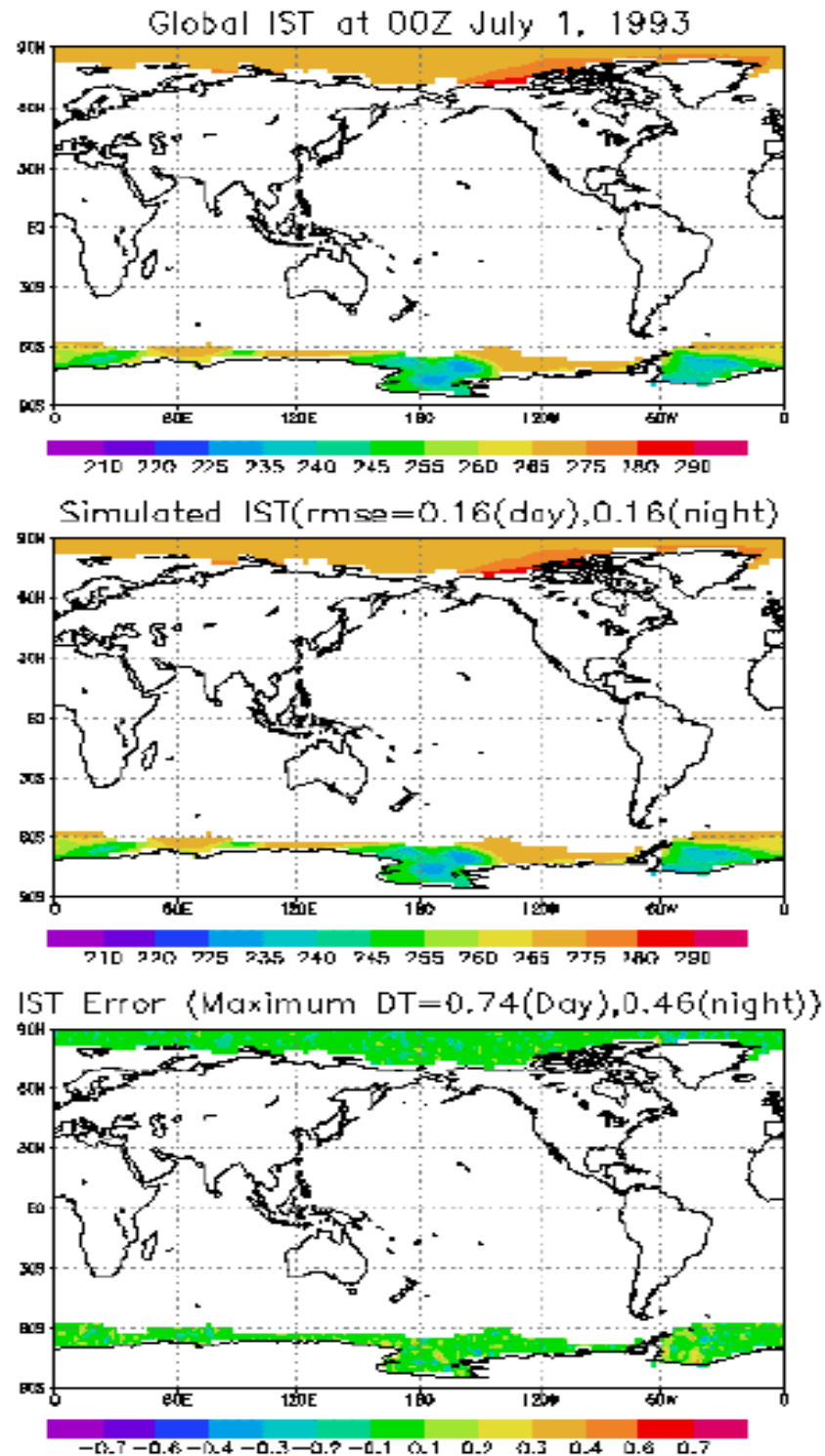


Figure 7. Upper panel: Global IST field. Middle panel: The retrieved IST values. Lower panel: The difference between the IST values.

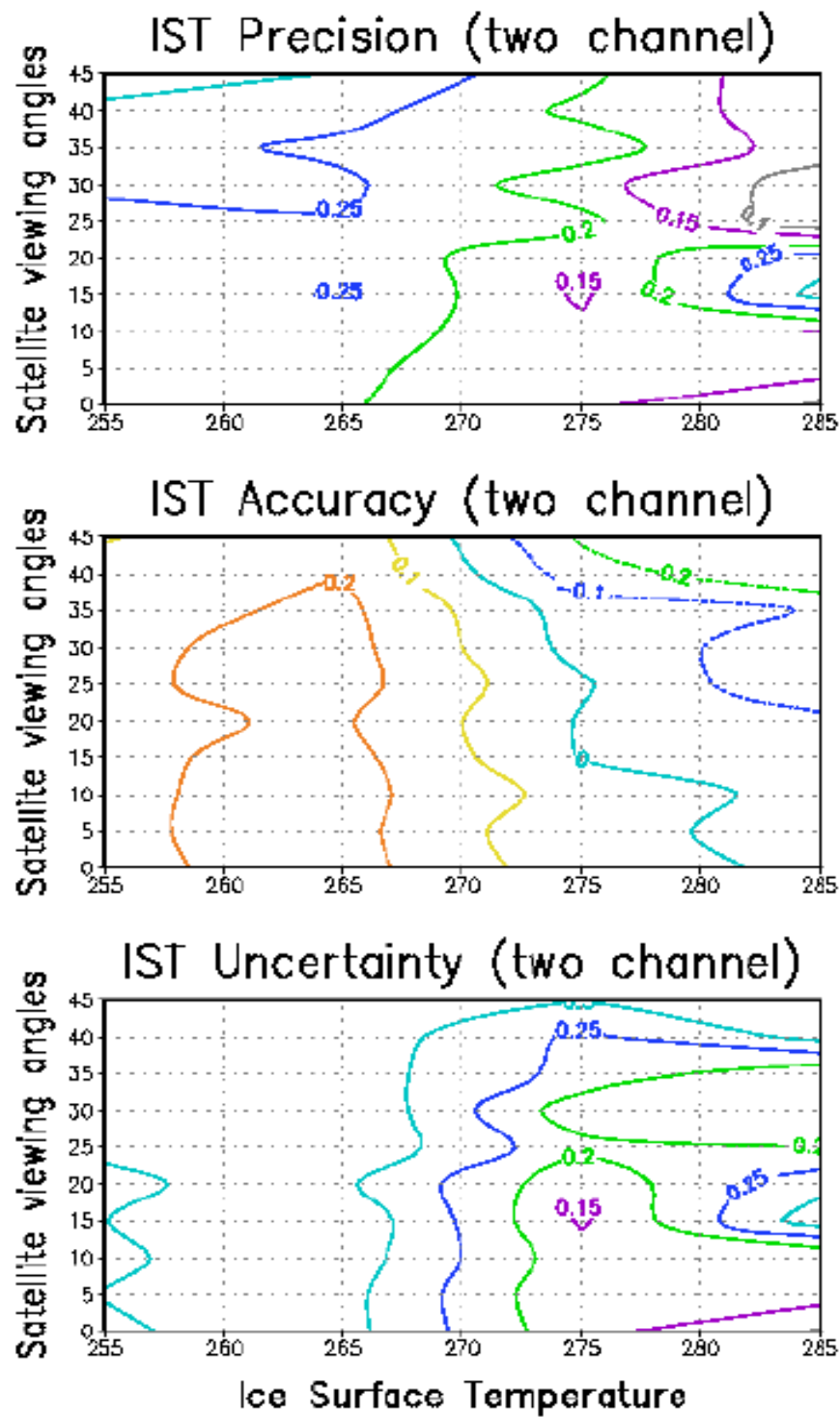


Figure 8. IST precision, accuracy, and uncertainty derived from the split window algorithms.

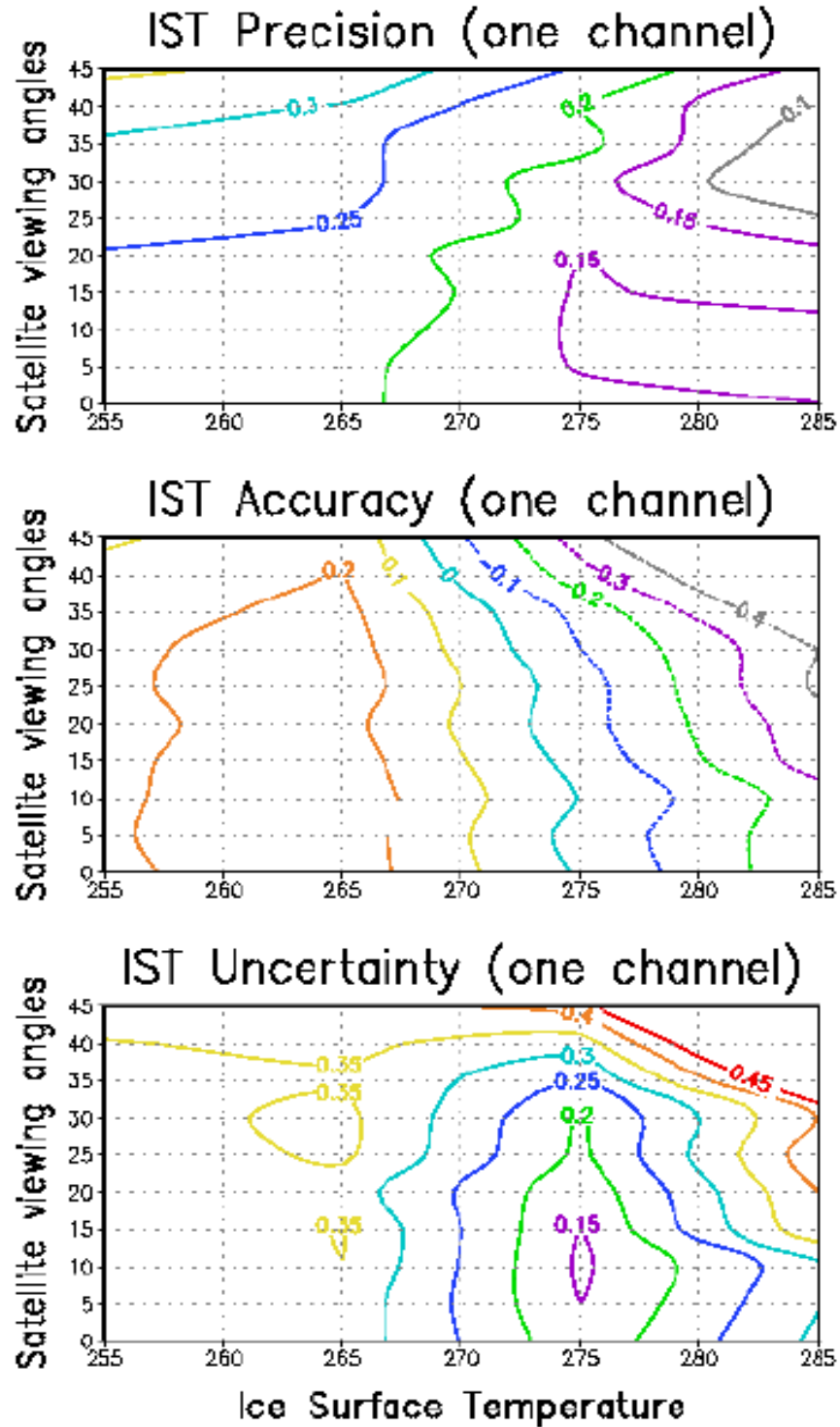


Figure 9. IST precision, accuracy, and uncertainty derived from the single band algorithms.

3.4 ALGORITHM SENSITIVITY STUDIES

3.4.1 Calibration Errors

We investigated the algorithm accuracy requirements relevant to the mean radiometric error in the sensor. We added mean errors to the simulated radiances and performed similar algorithms. Figure 10 shows how the accuracy changes with the mean error added to the radiance for each band. The data represents global observation. In order to meet 1.0 K accuracy, the calibration error for 11 and 12 micrometer bands must be less than 0.5 percent.

Split Window IST Accuracy vs. Calibration errors

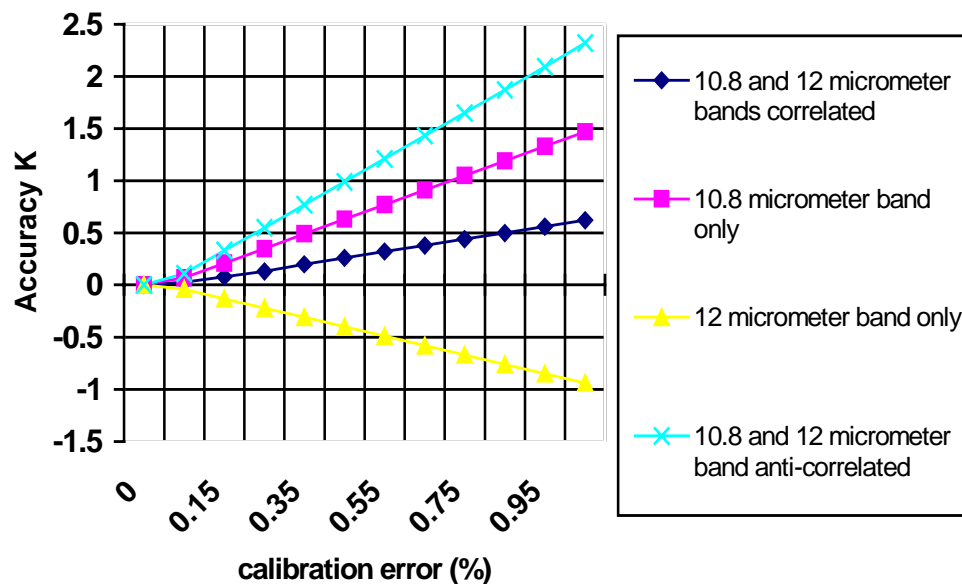


Figure 10. Split window IST accuracy related to calibration errors.

Figure 11 shows the IST accuracy for global retrieval with a 0.2 percent absolute calibration error. The mean error is less than 0.25 K for all categories. The mean error becomes larger as the noise increases for some of the temperature categories with fewer samples.

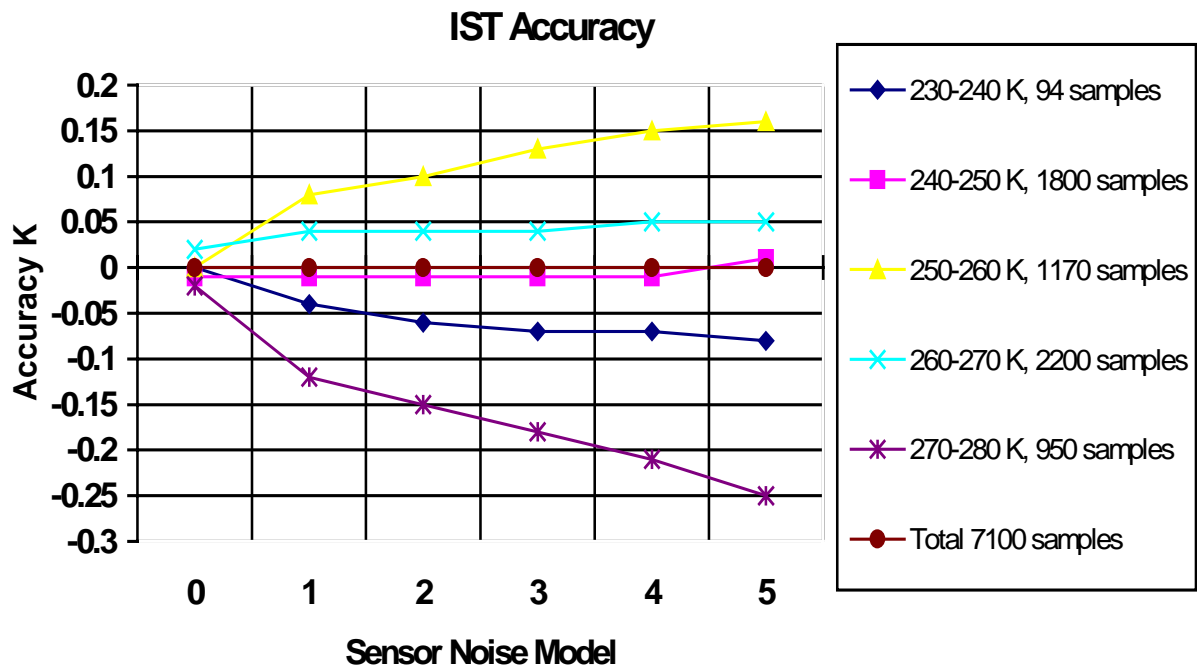


Figure 11. IST accuracy from global simulation

3.4.2 Instrument Noise

There are seven sensor noise models for the use of IST flowdown. They reflect seven different sensor aperture diameters, or NEDT values, for mid-IR and far-IR bands. Figure 12 shows the global IST uncertainties from simulations based on global snapshot skin temperatures and atmospheric profiles. The radiances were generated by MODTRAN 3.7. Noise was added to the simulated radiance through SBRS sensor noise models 1 through 5. Both noise and calibration errors were added to the testing data set. For the split window algorithm, the result for sensor noise model 3 is about 0.25 K in RMS error.

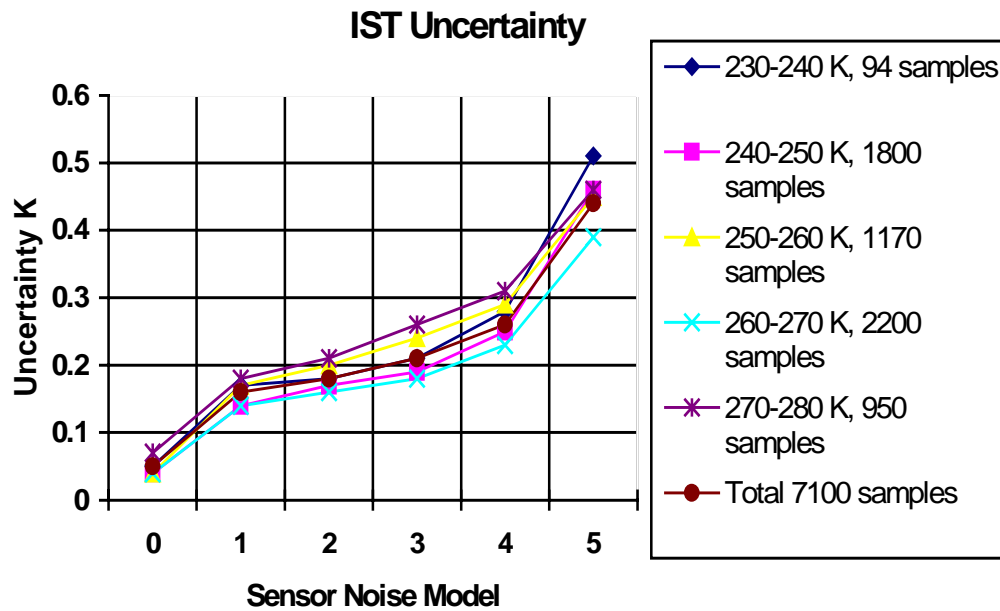


Figure 12. Global IST uncertainty for noise free case, and four sensor noise models, derived from testing data.

3.4.3 Ice Water Mixing

One of the area concerned is the ice/water mixed pixels. To estimate the error for the mixed region, both SST algorithm and IST algorithm were applied to two MAS scenes. In Figure 13, the left panel shows the ice surface temperature map, the middle panel shows the map of sea surface temperature and the right panel shows the difference. The difference map indicates that the surface temperatures retrieved using SST algorithm are generally higher than those derived from IST algorithm. But the difference is small (<0.5 K) over the ice surface. Over water, the difference can be as high as 1 K. Figure 14 is similar to Figure 13, but for another scene. The result is similar to that of the previous scene.

IST calculated using IST coefficients and SST coefficients

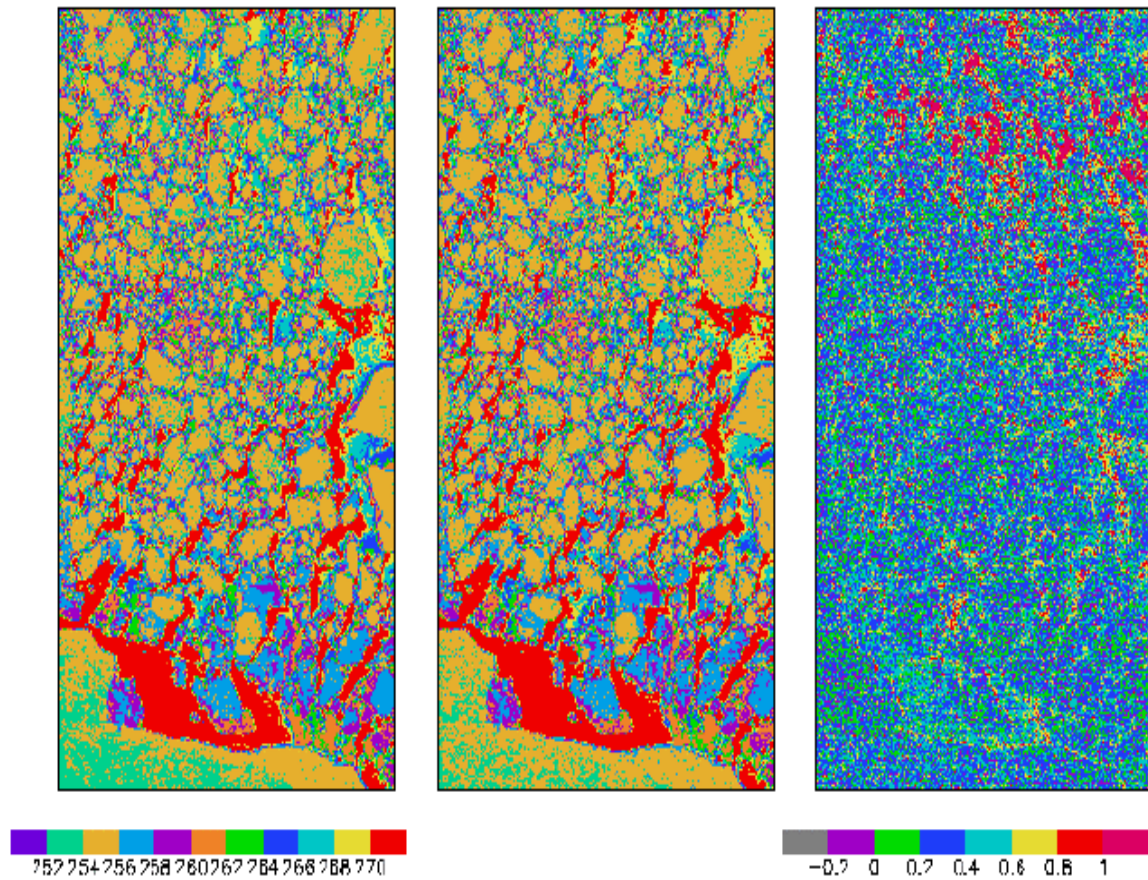


Figure 13. Left panel is the surface temperature derived using IST algorithm, middle is derived from the SST algorithm, and the right is the difference.

IST calculated using IST coefficients and SST coefficients

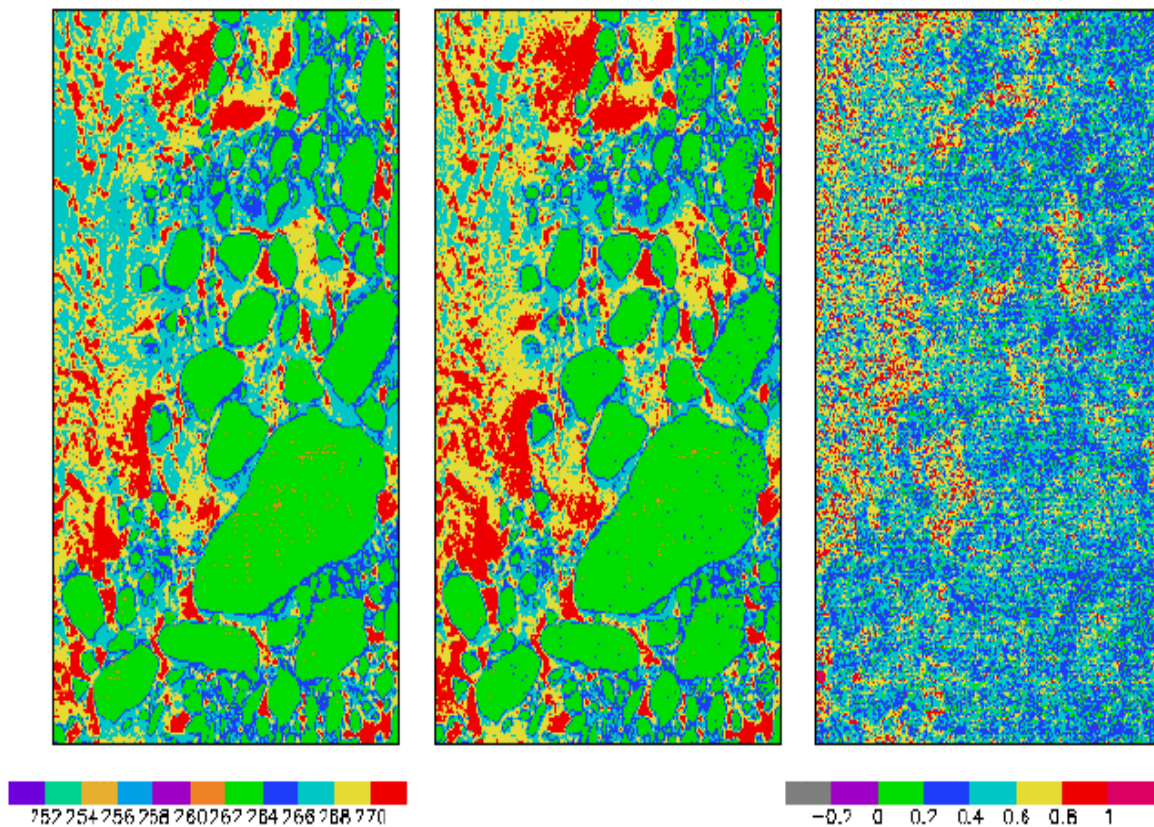


Figure 14. Left panel is the surface temperature derived using the IST algorithm, middle is derived from the SST algorithm, and the right is the difference.

3.4.4 Error Budget

Table 3 shows the ICT error budget. It indicates an uncertainty of better than 0.5 K for VIIRS IST retrieval.

Table 3. IST Error Budget

Ice Surface Temperature Specification v2 (Algorithm SFR)		Case: Global 2-bands				
5-May-99		Measurement				
		Accuracy	Precision	Uncertainty	Stability	Reference
Threshold		N/A	N/A	1.00	NA	SRD Version 2 Draft
Objective		N/A	N/A	0.30	NA	SRD Version 2 Draft
A-Specification		0.35	0.35	0.50	0.20	Raytheon Specification v2
Predicted Performance		0.30	0.32	0.44	0.14	Raytheon Specification v2
Margin		0.18	0.14	0.24	0.06	Raytheon Specification v2
Algorithm B-Specification		0.26	0.25	0.36	0.00	Raytheon Specification v2
Atmospheric Correction		0.06	0.15	0.16	0.00	2-bands
Forward Model		0.05	0.10	0.11	0.00	
Aerosols		0.10	0.10	0.14	0.00	10 km Visibility
Cloud Mask Errors		0.20	0.10	0.22	0.00	1%
Optically Thin Cirrus		0.10	0.10	0.14	0.00	0.2 optical thickness
Sensor B-Specification		0.15	0.20	0.25	0.14	Raytheon Specification v2
NEdT		0.00	0.15	0.15	0.00	Sensor Noise Model 3
BBR&MTF		0.00	0.10	0.10	0.00	20% IFOV MTF Model 5
Mapping Uncertainty		0.00	0.10	0.10	0.00	20% IFOV
Absolute Calibration		0.15	0.00	0.15	0.14	0.40% of TOA radiances

3.5 PRACTICAL CONSIDERATIONS

3.5.1 Numerical Computation Considerations

In order to stay current, an average processing of 10,000 pixels per second must be applied. Specific aspects of the implementation include calculation of the black body temperature. A counts-to-temperature look-up table will be used to speed the process. Physical retrievals need to run radiation transfer models. The current computer may only process a few pixels per second. Therefore, the physical retrieval will depend on the development of improved computer techniques.

3.5.2 Programming and Procedural Considerations

Look-up tables will be used to increase the computational efficiency. Registration and re-sampling into horizontal cell size will be made after the level 2 IST processing. Parallel processing is allowed for the IST retrieval.

All procedures will be automatic.

3.5.3 Configuration of Retrievals

An IST retrieval configuration is used to establish the numerical values of adjustable parameters used in the retrievals. This avoids hard-wiring specific values into the software.

3.5.4 Quality Assessment and Diagnostics

A number of parameters and indicators will be reported in the IST product as retrieval diagnostics. IST maps and statistical information will be reviewed for quality assessment. Quality flags will be provided which indicate the confidence in the IST processing. These will be determined by comparing IST values from different algorithms (e.g., regression and physical retrievals, or different regression methods).

3.5.5 Exception Handling

Cloud pixels identified by the cloud mask will be skipped. Pixels with bad data will also be skipped and flagged.

3.6 ALGORITHM VALIDATION

3.6.1 Pre-Launch Validation

The atmospheric correction algorithm will be derived pre-launch by radiative transfer modeling to simulate the VIIRS infrared channel measurements. Selected radiosoundings from the operational network stations or field campaigns will be used in VIIRS simulation for the development of the atmospheric correction algorithm. Measurements from the operational surface drifting and fixed buoy programs will be used to characterize the surface temperature fields and to validate the atmospheric correction algorithms. The assimilated meteorological fields provided by NCEP and European Center for Medium-Range Weather Forecast (ECMWF) provide a valuable description of the marine atmosphere and surface temperatures. These fields will be used in conjunction with the radiative transfer modeling to simulate the VIIRS measurements, to validate the radiosounding data and to provide direct input to the radiative transfer modeling process.

Measurements from AVHRR and ATSR will be used in the pre-launch phase to study the error characteristics of the IST retrieval.

3.6.2 Post-Launch Validation

The infrared channels of VIIRS form a self-calibrating radiometer. The infrared measurements are calibrated by using measurements of cold space and on-board black body targets. This produces radiance in the spectral intervals defined by the system response functions of each channel. These calibrated radiances can be converted to brightness temperatures at the height of the satellite. To derive IST from the calibrated radiance at satellite height, it is necessary to correct the effects of the intervening atmosphere.

The post-launch validation activities are designed primarily to test the efficiency of the IST retrieval algorithm. Several fundamentally different data sets are needed to provide an adequate sampling of the atmospheric conditions and IST to validate the VIIRS IR radiance and retrieved IST fields. Highly focused field expeditions are necessary to understand the atmospheric processes that limit the accuracy of the retrieved IST. Long-term global data sets are necessary to provide a monitoring capability that would reveal calibration drift and the consequences of extreme atmospheric events. Validation is required over the lifetime of the NPOESS missions.

The validation of IST is achieved using *in situ* measurements taken from thermistors or portable radiometers.

3.7 ALGORITHM DEVELOPMENT SCHEDULE

During this period, IST algorithms are mainly used to flowdown the sensor requirements. It is expected that this algorithm will be completed within 2 to 3 years.

4.0 ASSUMPTIONS AND LIMITATIONS

A major limitation of the VIIRS Ice Surface Temperature retrieval is that it can only be done under clear sky conditions. The algorithm is based on this basic assumption.

5.0 REFERENCES

- Berk, A., L. S. Bernstein, and D. C. Robertson (1987). MODTRAN: A moderate resolution model for LOWTRAN. Rep. GLTR-89-0122, Burlington, MA: Spectral Sciences, Inc.
- Cornette, W. M., P. K. Acharya, D. C. Robertson, and G. P. Anderson (1994). Moderate spectral atmospheric radiance and transmittance code (MOSART). Rep. R-057-94(11-30), La Jolla, CA: Photon Research Associates, Inc.
- Key, J., J. A. Maslanik, T. Papakyriakou, M. C. Serreze, and A. J. Schweiger (1994). On the validation of satellite-derived sea ice temperature. *Arctic*, 47, 280-287.
- Kneizys, F. X., E. P. Shettle, L. W. Abreu, J. H. Chetwynd, G. P. Anderson, W. O. Gallery, J. E. A. Selby, and S. A. Clough (1988). Users guide to LOWTRAN7. Rep. AFGL-TR-88-0177, Bedford, MA: Air Force Geophys. Lab.
- Yu, Y., D. A. Rothrock, and R. W. Lindsay (1995). Accuracy of sea ice temperature derived from the advanced very high resolution radiometer. *J. Geophys. Res.*, 100, 4525-4532.